Available online at www.sciencedirect.com

SciVerse ScienceDirect

Procedia Engineering 42 (2012) 1692 – 1710

Procedia Engineering

www.elsevier.com/locate/procedia

20th International Congress of Chemical and Process Engineering CHISA 2012
25 – 29 August 2012, Prague, Czech Republic

Solution of inverse problem with the one primary and one secondary particle model (OPOSPM) coupled with computational fluid dynamics (CFD)

H. B. Jildeh[a,b], M. W. Hlawitschka[a,b], M. Attarakih[a,c], H. J. Bart[a,b] a*

[a]*Chair of Separation Science and Technology, TU Kaiserslautern, P.O. Box 3049 - 67653 Kaiserslautern, Germany*
[b]*Centre of Mathematical and Computational Modelling, TU Kaiserslautern, P.O. Box 3049 - 67653 Kaiserslautern, Germany*
[c]*Department of Chemical Engineering, The University of Jordan, 11942 Amman, Jordan*

Abstract

The reduced one group population balance (PBE) model, the One Primary and One Secondary Particle Model (OPOSPM) is developed for a liquid extraction column. It is used because of its simplicity and the ability to reproducemost of the information contained in the PBE. It is usedto estimate the optimum droplet breakage and coalescence parameters using steady state experimental data. The data is obtained from a pilot plant liquid extraction column of 80 mm diameter and 4.4 m height for toluene-acetone-water chemical test system as recommended by the European Federation of Chemical Engineering (EFCE). In this contribution Coulaloglou and Tavlarides (1977)breakage and coalescence model is studied to obtain the parameters by solving a population balance inverse problem. The estimated droplet parameters are used as input parameters for the CFD simulation and in the simulation program PPBLAB.The optimized values were found to predict accurately the mean dispersed phase holdup, mean droplet diameter and the concentration profile for the continuous and dispersed phase along the extraction column height.

Keywords: Population balance; inverse problem; hydrodynamics; breakage; coalescence; extraction column; RDC; modeling

*Corresponding author. Tel.: +49-631-205-2414; fax: +49(0)631-205-2119.
E-mail address: bart@mv.uni-kl.de.

doi:10.1016/j.proeng.2012.07.562

Nomenclature

A	specific surface area
A_c	column cross-sectional area
C_D	drag coefficient
C_n	adjustable parameters
c	solute concentration
D	diffusion coefficient
d	droplet diameter
d_{30}	volumetric diameter
F	forces
$f(x, t)$	density function
G_k	turbulence kinetic energy
G_n	constants
g	gravitational constant
h	collision rate frequency
K	mass transfer coefficient
K_{pq}	interphase momentum exchange coefficient
K_{oy}	overall mass transfer coefficient
k	kinetic energy
m	swarm exponent
m^*	distribution coefficient
$\dot{m}_{pq}$	mass transferred between the two phases
N	number concentration
p	pressure
Pe	Péclet number
Q	volumetric flow rate
R	interaction term
$\dot{R}(x,t)$	velocities for internal coordinate
Re	Reynolds numbers
S	source term

Sc	Schmidt number
Sh	Sherwood number
t	time
u	droplet velocity
V_t	terminal velocity
$\dot{X}(x,t)$	velocities for external coordinate
$x_{i,j}$	coordinate
y^+	wall distance unit
z	space coordinate

Greek letters

α	phase fraction (volume concentration)
Γ	breakage frequency
ε	energy dissipation
η	dynamic viscosity
λ	coalescence efficiency
ρ	density
σ	surface tension
σ_k	Prandtl number for kinetic energy
σ_ε	Prandtl number for energy dissipation
τ	stress tensor
v	droplet volume
Υ	source term
φ_d	holdup fraction
ψ	internal and external coordinates vector [$d\ c_y\ z\ t$]
ω	coalescence rate
ϑ	mean number of daughter droplets

Subscripts

in	inlet (feed)
n	number of parameters:1…4 or constants 1ε and 2ε
p	phase 1
q	phase 2

t	turbulent
x	continuous phase
y	dispersed phases

Superscript

*	equilibrium
‘	turbulence
i	component
in	inlet

1. Introduction

In the past decade the demand on the simulation of chemical process equipment is increased to save time and money by exploring operational conditions that are not easily achievable in laboratory scale devices. One of the industrially important processes is liquid-liquid extraction, which is widely used when distillation is economically infeasible or can damage the chemical components to be separated and is commonly used in mining, petroleum, chemical and biochemical industries. Therefore simulation of liquid extraction equipment is vital for equipment scale-up, model predictive control and optimization. However, due to theirs complex hydrodynamics it is difficult to predict theirs performance using simple mathematical models. Hence, a droplet population balance model (DPBM) should be used, which takes into account droplet transport (rise and backmixing) and droplet interactions at macro-scale (droplet breakage and coalescence) and micro-scale (interphase mass transfer). This DBPM is programmed and developed in order to simulate accurately the liquid-liquid extraction columns (LLECs) in a user-friendly environment such as LLECMOD (Liquid-Liquid Extraction Column MODule) [1, 2, 3], which is now available in a MATLAB interface named as PPBLAB(Particulate Population Balance LABoratory) [4].

A disadvantage of this approach is its sensitivity to geometrical constraints and the necessity to use correlations valid for a certain geometry. For example, the dispersion coefficients, Weber numbers which can all be directly derived independent from geometric constraints when using Computational Fluid Dynamics (CFD). First simulations of a coupled CFD-DPBM simulation of a full pilot plant Rotating Disk Contactor (RDC) were done by Drumm et al. (2010) [5] using a one group model, called one primary and one secondary particle model (OPOSPM), whereas the breakage and coalescence parameters were adjusted by hand to the test system. For mass transfer simulations, a correct determination of the droplet size and interfacial area is essential to predict the correct concentration profiles and its influence on the hydrodynamics. This droplet size undergoeschanges after entering the extraction column due to droplet breakage and coalescence. Due to the high computational time of a CFD-DPBM-mass transfer simulation, a determination of the droplet interaction parameters by trial and error is not suitable or even appropriate. In order to obtain the correct parameters, which must be known at the beginning of a simulation, a solution of a population balance inverse problem is necessary as well bediscussed below.

As test case, a pilot plant RDC extraction column of 80 mm diameter and 4.4 m height which wasexperimentally investigated by Garthe (2006) [6] was chosen. Hence, the required correlations for e.g. the droplet rise velocity are given and can be directly used to determine the correct DPBM parameters for

the measured holdup profile using the inverse problem without further experiments and simulations. These parameters are then used for a coupled CFD-DPBM-mass transfer simulationusing the commercial CFD code Fluent. The resulting droplet size, holdup and concentrations along the column height are compared to the experimental data and simulations with PPBLAB.

2. Population Balance Model

The general population balance equation (PBE) and its derivation based on Reynolds transport theory is given in Ramkrishna (2000) [7]. It is based on the deforming particle space continuum, which assumes that particles are embedded in this continuum at every point such that the distribution of particles is described by a continuous density function *f(x, t*), and expressed by the following equation:

$$\frac{\partial f(x,t)}{\partial t} + \nabla_x \cdot (\dot{X} f) + \nabla_r \cdot (\dot{R} f) = S \qquad (1)$$

where$\dot{R}(x,t)$, $\dot{X}(x,t)$are the velocities for internal and external coordinates respectively. Thus $\dot{R}(x,t)f(x,t)$ is the particle flux through internal coordinate space (concentration, droplet diameter, color, etc.) and $\dot{X}(x,t)f(x,t)$ is the particle flux through physical space. *S*is an integral expression source term, which depends on the specific processes by which particles appear and disappear from the system (particle breakage, aggregation, growth and nucleation) and is given in detail in Ramkrishna (2000) [7]. This model has been used widely for modeling and simulating in different chemical processes such crystallization, precipitation (protein precipitation), gas-liquid (bioreactors, evaporation) andgas-solid (fluidized bed reactors)processing and in polymerization.

2.1. Mathematical model

This general model has been adapted for LLECs to couple hydrodynamics and mass transfer in a one spatial domain by using the Multivariate Sectional Quadrature Method Of Moments (MSQMOM). The general spatially distributed population balance equation (SDPBE) can be presented by [1, 2, 8]:

$$\frac{\partial f_{d,c_y}(\psi)}{\partial t} + \frac{\partial \left[u_y f_{d,c_y}(\psi) \right]}{\partial z} + \frac{\partial \left[\dot{c}_y f_{d,c_y}(\psi) \right]}{\partial c_y} = \frac{\partial}{\partial z}\left[D_y \frac{f_{d,c_y}(\psi)}{\partial z} \right] + \frac{Q_y^{in}}{A_c} f_y^{in}(d, c_y; t)\delta(z - z_y) + \Upsilon\{\psi\} \qquad (2)$$

At the left hand side of the equation is the transient term, convection term and diffusion term, where the velocity along the concentration coordinates (c_y) is ($\dot{c}_y$). The source terms are described on the right hand side of the equation. The first source term describes the droplet axial dispersion characterized by the dispersion coefficient D_y, which dependent on the energy dissipation, holdup and droplet rise velocity. The second one expresses droplet entering rate to LLEC with a volumetric flow rate Q_y^{in} that is perpendicular to column cross sectional area A_c at a location z_y with an inlet number density f_y. The third one (Υ) represents the net number of droplets produced by breakage and coalescence per unit volume and unit time, which represents the four rates of droplet birth (B) and death (D) due to breakage (b) and coalescence (c) in a turbulent continuous phase:

$$\Upsilon\{\psi\} = B^b(d,c_y;t,z) - D^b(d,c_y;t,z) + B^c(d,c_y;t,z) - D^c(d,c_y;t,z) \quad (3)$$

In this equation the components of the vector ψ = *[d c_y z t]* are those for the droplet internal bivariate coordinates: the droplet diameter (*d*), solute concentration (c_y) and the external coordinate: the location (*z*) and time (*t*). The four rates are given by set of equations which are presented in Attarakih et al. (2008) [2].

2.2. Numerical methods

In technical geometries the population balance model (PBM) has no general analytical solution; therefore the only choice in most cases is a special numerical technique to solve the PBE. Several numerical approaches are proposed to solve the PBE which are classified into the following categories: Classes method (CM), Monte Carlo method (MCM) and method of moments (MOM).

The Classes methodis known also as direct discretization method (DDM).In this method the internal coordinate is discretized in the solution domain using a traditional discretization method such as finite difference method, finite element method or finite volume method directly.This method is straightforward; it gives the full particle size distribution with a good accuracy. In some cases to achieve a good accuracy a large number of classes has to be used, that will require large number of equations to be solved.This method is used in commercial CFD software (CFX, FLUENT), however, it needs a long computational time and it preserves only two integral properties of the distribution asKumar and Ramkrishna proposed in the fixed pivot discretization method and the moving pivot technique [9,10].

On the other hand, the Monte Carlo method is a stochastic method that involves the construction of an artificial system to approximate the actual one based on the physical characteristics of the considered system [11]. There are two classifications concerning this method. First, it can be divided into time and event driven algorithms according to the driven pattern of the discrete physical events [11, 12]. Second, it can be classified into constant volume and constant number methods according to the state of the particles in the artificial system. To decrease the statistical errors a very large number of particles are required and this will need a high computational time. The numerical results from this method usually contain ``noises´´, for these reasons it is difficult to be coupled with a CFD code.

The method of moments has been widely used because of its efficiency and high accuracy also when it is coupled with CFD code FLUENT [5, 13]. In this method the particle size distribution is not tracked directly but through its moments, which are integrated over the internal coordinates. It needs a very low computational time. However this method does not give information on the shape of the distribution. JunWei et al. (2009) has provided a brief literature review for different methods of MOM such as [11]: Quadrature Method Of Moments (QMOM), Direct Quadrature Method Of Moments (DQMOM), Modified Quadrature Method Of Moments (M-QMOM), Adaptive Direct Quadrature Method Of Moments (ADQMOM), Fixed Pivot Quadrature Method Of Moments (FPQMOM), Local Fixed Pivot Quadrature Method Of Moments (LFPQMOM) and etc. In 2009,Attarakih has invented a new technique for the QMOM to solve of PBE using the Sectional Quadrature Method Of Moments (SQMOM), which combines the advantages of CM and MOM in one model with high accuracy, low computational time and without destroying the shape of the distribution [14]. This model is based on primary and secondary particle concept which will be discussed in the next section. Then the SQMOM model was extended to the Bivariate Sectional Quadrature Method Of Moments (BVSQMOM) and the Multivariate Sectional Quadrature Method Of Moments (MSQMOM) [15]. Later this model has been extended to the Cumulative Quadrature Method Of Moments (CQMOM) [16] and the Normalized Quadrature Method Of Moments (NQMOM) [17].

2.2.1. One Primary and One Secondary Particle Model (OPOSPM)

The One Primary One Secondary Particle Method is the simplest discrete model case of the SQMOM that can approximate the continuous PBE [2]. It provides a promising one group reduced PBM that reduces the computational time. This model is based on the primary and secondary particle concept, where the primary particles are responsible for reconstruction of the distribution and the secondary particle is to describe the particle interaction due to breakage and coalescence [18].

$$\frac{\partial N}{\partial t}+\frac{\partial(u_y N)}{\partial z}=\frac{1}{A_c}\frac{Q_y^{in}}{\upsilon_{in}}\delta(z-z_y)+S \tag{4}$$

$$\frac{\partial \alpha}{\partial t}+\frac{\partial(u_y \alpha)}{\partial z}=\frac{Q_y^{in}}{A_c}\delta(z-z_y) \tag{5}$$

This model is able to capture all the essential physical information contained in the PBM and is still tractable from computational point of view. The model conserves the total number (N) and volume (α) concentrations of the population by solving directly two transport equations for N and α. The source term S represents the net number of the droplets and is expressed by the following equation:

$$S=(\vartheta(d_{30})-1)\Gamma(d_{30})N-\frac{1}{2}\omega(d_{30},d_{30})N^2 \tag{6}$$

The first term is the rate of droplet formation due to breakage, and is expressed in terms of the breakage frequency Γ. ϑ is the mean number of daughter droplets that is determined by integrating the daughter droplet distribution function, in the simulation it is assumed equal to 3 (mother droplet breakup to form three daughter droplets). The second term represents the net rate of droplet death due to coalescence, and expressed as the coalescence frequency ω. Both breakage and coalescence frequencies are function of droplet size, energy dissipation and system physical properties (density, viscosity andsurface tension).d_{30} is the mean diameter and is given as the ratio between volume and number concentrations.

$$d_{30,i}=\sqrt[3]{\frac{6}{\pi}\frac{\alpha_i}{N_i}} \tag{7}$$

The OPOSPM model is used to simulate the droplet size distribution based on the model of Coulaloglou and Tavlarides (1977) [19] for breakage and coalescence in the CFD simulation using the optimized parameters obtained from the solving inverse population balance problem.

3. Phenomena Affecting Droplet Size

The droplet population balance model (DPBM) has to be used to predict the performance of liquid extraction columns that takes into account droplet transport and droplet interactions. Detailed description about theses phenomena will be discussed in the next sections.

3.1. Droplet velocity

In agitated columns there are two factorsgoverning drop motion: first the drop motion due to buoyancy force and the second is random drop motion due to flow instability [20]. Knowledge of the drop velocityis necessary for the prediction of holdup, the residence time and mass transfer rates of both phases. This is based on determining the relative swarm velocity and the effective phase velocity. The droplet velocity and the axial dispersion are considered the key parameter for calculating the drift term in the PBE.

Semi-empirical correlations are used to determine the drop velocity for various sizes and physico-chemical that are dependent on the chemical test system. For the high interfacial liquid system: toluene-acetone-water (our studied system) Vignes' lawis proposedand is given by the following equation [20]:

$$V_t = \frac{d}{4.2}\left(\frac{g\Delta\rho}{\rho_x}\right)^{2/3}\left(\frac{\rho_x}{\eta_x}\right)^{1/3} \tag{8}$$

On the other hand the characteristic velocity in stirred columns is controlled and modeled by the droplet size, geometry of the agitators and stators, and the energy input[6]. This general description is used for the optimization algorithm to describe the dispersed phase hydrodynamics, and also has been used in the PPBLAB simulations.

3.2. Droplet interactions

The droplet interactions occurat macro-scale (droplet breakage and coalescence) and micro-scale (interphase mass transfer).

3.2.1. Drop breakage

The deformation and breakup of fluid particles in turbulent dispersions is influenced by the continuous phase hydrodynamics and the interfacial surface tension. Also it is dependent on the droplet size, density, interfacial tension, viscosity of bothphases, holdup, local flow and energy dissipation [19]. Generally the breakage mechanism of the droplet can be classified into four main categories as are turbulent fluctuation and collision, viscous shear stress, shearing-off process and interfacial instability [21]. In literature different mechanisms exist and they are strongly dependent on the geometry, especially in liquid extraction columns with different stirring devices. For example the droplet breakup in Kühni column while passing through the turbine outlet stream, but in RDC extraction columns it occurs only when the droplet touch the rotator disc.

Several models exist in literature for droplet breakage, but here we will use the model of Coulaloglou and Tavlarides (1977) [19]. This model was based on the turbulent nature of liquid-liquid dispersion, where the drop oscillates and deforms due to the local pressure fluctuation. The breakage frequency $\Gamma(d)$is defined by the following equation[19, 21]:

$$\Gamma(d) = \left(\frac{1}{breakage\ time} \right) \cdot \left(\frac{fraction\ of}{drops\ breaking} \right) \tag{9}$$

The breakage time is determined by isotropic turbulence theory by assuming that the motion of daughter droplets is the same as turbulent eddies. On the other hand the fraction of drops breakage is assumed proportional to the fraction of drops that have a turbulent kinetic energy greater than their surface tension. Coulaloglou and Tavlarides (1977) relationship is based on the fundamental model of mixer hydrodynamics with taking into account the influence of holdup [19-21]:

$$\Gamma(d,\phi_d) = C_1 \frac{\varepsilon^{1/3}}{d^{2/3}(1+\phi_d)} \left[\exp\left(-\frac{C_2 \sigma (1+\phi_d)^2}{\rho_x d^{5/3} \varepsilon^{2/3}} \right) \right] \tag{10}$$

The number of daughter droplets produced by a single breakage event is assumed to be three in order to simplify the computational problems of modeling, in which the $\vartheta\ (d_{30}) = 3$ in Eq. (6).

3.2.2. Drop coalescence

Droplet coalescence is considered more complex then breakage because of the droplet interaction with the surrounding liquid phase and with other droplets when they are brought together by external flow and body forces. For coalescence of droplets to occur in a turbulent flow field the droplet first collide then remain in contact for sufficient time so that the processes of film drainage, film rupture and coalescence to occur. The droplets may separate caused by a turbulent eddy or adsorption layers, which prevent the coalescence [19]. Also the intensity of collision and the contacting time between the colliding droplets are the key parameters for this phenomenon.

There are several models in literature for coalescence of fluid particles for example Coulaloglou and Tavlarides (1977) [19], Sovova model (1981) [22], Casamatta and Vogelpohl (1985) [23], Laso (1986) [24], Lane (2005) [25],etc. A literature review has been done by Liao and Lucas (2010) for most of these models [26]. The physical models calculate the coalescence frequency from the product of collision rate (frequency) (h) and the coalescence efficiency (λ) of two droplets from diameter d and d'[26, 27].

$$\omega(d,d',\phi_d) = h(d,d',\phi_d)\ \ \lambda(d,d',\phi_d) \tag{11}$$

Coulaloglou and Tavlarides (1977) is one of the most used models because the derived model is based on the physical quantities of the chemical test system, therefore it is the one we choose for our optimization [26]. This model was developed for stirred vessel, being based on the kinetic theory of gases and drainage film theory. It is given by the following equation:

$$\omega(d,d',\phi_d) = \left[C_3 \frac{\varepsilon^{1/3}}{1+\phi_d} (d+d')^2 (d^{2/3}+d'^{2/3})^{1/2} \right] \times \left[\exp\left(-\frac{C_4 \eta_x \rho_x \varepsilon}{\sigma^2 (1+\phi_d)^3} \right) \left(\frac{(dd')}{(d+d')} \right)^4 \right] \tag{12}$$

In this model the first term is the collision rate frequency of two droplets. It can be described in analogy to collision frequency between gas molecules of drop diameter *d* and *d'* for size intervals *Δd* and *Δd'*. In this term the influence of the holdup is considered as a damping effect on turbulent velocities [19, 20]. On the other hand the second term is thefraction of collisions between drops of size *d* and *d'* that result in a coalescence is known as coalescence efficiency. It accounts for the contact time between two droplets and the coalescence time. Unusually in this phenomenon the contact time must exceed the coalescence time, after collision [6, 19]. Furthermore, the coalescence efficiency for this model is classified for deformable particles with immobile interfaces and the initial and final film thickness are assumed to be constant.

3.2.3. Mass Transfer

The mass transfer influences on the resulting hydrodynamics behavior and is affectedby the mass transfer direction from continuous to disperse or vice versa[20]. The solute concentration in the continuous phase (c_x) is predicted using a component solute balance on the continuous phase [2]:

$$\frac{\partial(\phi_x c_x)}{\partial t}-\frac{\partial}{\partial z}\left(u_x\phi_x c_x+D_x\frac{\partial(\phi_x c_x)}{\partial z}\right)=\frac{Q_x^{in}c_x^{in}}{A_c}\delta(z-z_y)-\int_0^{\infty}\int_0^{c_{y,\max}}\dot{c}_y v(d)f_{d,c_y}(\psi)\partial d\partial c_y \qquad (13)$$

The volume fraction of the continuous phase (φ_x) satisfies the physical constraint:$\varphi_x+\varphi_y=1$. The left hand side and the first term on the right hand side have the same interpretations as those given in Eq.(2); however, with respect to the continuous phase. Whereas the last term represents the total rate of solute transferred from the continuous to the dispersed phase, in which the liquid droplets are treated as point sources.

The overall mass transfer coefficient (K_{oy})which can be used to predict the rate of change of solute concentration in the liquid droplet is expressed in terms of the droplet volume average concentration:

$$\frac{\partial c_y(z,t)}{\partial t}=\frac{6K_{oy}}{d}\left(c_y^{*}(c_x)-c_y(z,t)\right) \qquad (14)$$

The$K_{oy}$is a function of the droplet diameter and time depending on the internal state of the droplet. This coefficient is usually expressed using the two-resistance theory in terms of the individual mass transfer coefficients for the continuous and the dispersed phases. In agitated columns the energy input increases the mass transfer by a forced circulation of the drops in the compartments and by induced circulations within the drops.

4. Parameter Estimation

Inverse problems are ill-posed in general and need some stabilization techniques to get reliable optimized parameters. It is considered complicated due to the increase in the size of the differential algebraic system when dealing with the inverse problem using the population balance models. Depending on experimental data availability and in particular in industrial cases where only few intermediate data along the equipment height are available. In some cases only the inlet and outlet mean properties are available. Therefore, the DPBM for coupled hydrodynamics and mass transfer has to be solved. Accordingly, not only the size of the system is considerably increased, but also the computational time

due to the slow mass transfer process. Also the resulted equations should be solved simultaneously; therefore this calls for efficient mathematical modeling and a proper algorithm design. Besides to this, solving the population balance inverse problem and getting a converging solution in a short time is found to be highly sensitive to errors in the experimental data.

Consequently, the recent developed model by Attarakih et al. [18]: the One Primary and One Secondary Particle Model (OPOSPM) is found to provide a promising one group reduced PBM that can be used to solve the inverse population balance problem.The solution of the inverse problem is formulated as a nonlinear optimization problem, which is constrained by simple bounds on both the breakage and coalescence parameters in order to obtain the correct scale for the model of Coulaloglou and Tavlarides[19] in an RDC and Kühni extraction column [28, 29]. The algorithm has been programmed using MATLAB, for optimization of coalescence parameters the tolerance was set to 1.00E-6. The objective of this work is not to fit the experimental data but also to check whether the optimized parameters can predict the steady state and dynamic behavior of the liquid extraction column under other operating conditions. Obtaining these parameters is used as a basis for the CFD. TheOPOSPM is used effectively to simulate the full column hydrodynamics and mass transfer.

5. Computational Fluid Dynamics

In comparison to the optimization tool and PPBLAB, CFD is able to calculate the flow field without geometrical based correlations e.g. for the droplet rise velocity. The commercial CFD code FLUENT (v121) was coupled with the previously described OPOSPM model to account for breakage and coalescence. Likewise in PPBLAB the breakage and coalescence of the droplets is accounted by the model of Coulaloglou and Tavlarides [19] using the estimated parameters from the inverse problem. In addition, mass transfer is accounted to simulate the concentration profile along the column height of an RDC pilot plant extraction column.

5.1. Hydrodynamics

The two phases are treated as interpenetrating continua using the Euler-Euler framework. Hence, the phases are described by the phase fraction in each cell, whereas the sum of the volume fraction α of all phases q in each cell has to be 1:

$$\sum_{p=1}^{n} \alpha_q = 1 \tag{15}$$

The transport of the phases is described by the continuity equation for each phase:

$$\frac{d}{dt}\left(\alpha_q \rho_q\right) + \nabla\left(\alpha_q \rho_q \vec{u}_q\right) = \sum_{p=1}^{n} \dot{m}_{pq} \tag{16}$$

Hereby, the density of phase q is described by ρ_q and the velocity of each phase by $\vec{u}_q$. The right hand side of the equation describes the mass transfer from phase p to q, which is described as source term. The conservation equation for each phase is given by:

$$\frac{d}{dt}\left(\alpha_q \rho_q \vec{u}_q\right) + \nabla\left(\alpha_q \rho_q \vec{u}_q \vec{u}_q\right) = -\alpha_q \nabla p + \nabla \bar{\bar{\tau}}_q + \alpha_q \rho_q g + \sum_{p=1}^{n}\left(\vec{R}_{pq} + \dot{m}_{pq}\vec{u}_q\right) + \alpha_q \rho_q \vec{F} \quad (17)$$

where the pressure is described by $p$and the stress tensor is described by $\bar{\bar{\tau}}_n$. The interaction term$R_{pq}$is defined as:

$$\sum_{p=1}^{n} \vec{R}_{pq} = \sum_{q=1}^{n} K_{pq}\left(\vec{u}_p - \vec{u}_q\right) \quad (18)$$

with K_{pq} as the interphase momentum exchange coefficient:

$$K_{pq} = \frac{3\alpha_q \alpha_q \rho_q \left|\vec{u}_p - \vec{u}_q\right| C_D}{4\, d} \quad (19)$$

The drag coefficient C_D is taken from Schiller and Naumann:

$$C_D = \begin{cases} 24\left(1 + 0.15\, Re^{0.687}\right)/Re & Re \leq 1000 \\ 0.44 & Re > 1000 \end{cases} \quad (20)$$

The density of each phase is given by the concentration of the transferred component and the density of each component:

$$\rho_{q,m} = \rho_{q,1}\left(1 - c_q^t\right) + \rho_{q,2} c_q^t \quad (21)$$

5.1.1. Mass transfer

The concentration of the transferred component has to be tracked in the whole domain. This is done using the species transport equations in FLUENT [30]:

$$\frac{d}{dt}\left(\alpha_q \rho_q c_q^t\right) + \nabla\left(\alpha_q \rho_q \vec{u}_q c_q^t\right) = \alpha_q S_q^t \quad (22)$$

The mass transfer of the transferred component is accounted by the source term, whereas in this case, the source term is based on the two film theory:

$$\dot{m} = A \rho_q \rho_{pq} K_{oy}\left(m^* c_q^t - c_p^t\right) \quad (23)$$

where m^* is the distribution coefficient. The interfacial area$A$is calculated based on the phase fraction and the diameter of the droplets:

$$A = \frac{6\,\alpha}{d} \tag{24}$$

The overall mass transfer coefficient describes the diffusion rate across the surface of the droplets and is based on the individual mass transfer coefficients of the continuous phase K_x and dispersed phase K_y:

$$\frac{1}{K_{oy}\rho_y} = \frac{1}{K_y\rho_y} + \frac{m}{K_x\rho_x} \tag{25}$$

To determine the individual mass transfer models, the model of Kumar and Hartland (1999) was used for both the CFD and PPBLAB simulations and is given by the following equations [31]:

$$K_x = \frac{D_x}{d}\cdot\frac{Sh_{x,\infty}\cdot\alpha + Sh_{x,rigid}}{1+\alpha} \text{ with } Sh_{x,\infty} = 50 + \frac{2}{\pi^{0.5}}\cdot Pe_x^{0.5} \text{ and } Pe_x = \frac{d\cdot u}{D_x} \tag{26}$$

where $Sh_{x,rigid}$ and α defined as:

$$Sh_{x,rigid} = 2.43 + 0.775\cdot Re^{0.5}\cdot Sc_x^{\frac{1}{3}} + 0.0103\cdot Re\cdot Sc_x^{\frac{1}{3}} \tag{27}$$

$$\alpha = 5.26\times 10^{-2} Re^{\frac{1}{3}+6.59\times10^{-2}Re^{\frac{1}{4}}} \times Sc_x^{\frac{1}{3}}\left(\frac{u\,\eta_x}{\sigma}\right)^{\frac{1}{3}}\frac{1}{1+\left(\eta_y/\eta_x\right)^{1.1}} \tag{28}$$

where:

$$Re = \frac{\rho_x\,u\,d}{\eta_x} \text{ and } Sc_x = \frac{\eta_x}{D_x\rho_x} \tag{29}$$

$$K_y = \frac{D_y}{d}\cdot Sh_y, \quad Sh_y = 17.7 + \frac{3.19\times10^{-3}\left(Re\,Sc_y^{\frac{1}{3}}\right)^{1.7}}{1+1.43\times10^{-2}\left(Re\,Sc_y^{\frac{1}{3}}\right)^{0.7}}\left(\frac{\rho_y}{\rho_x}\right)^{\frac{2}{3}}\times\frac{1}{1+\left(\eta_y/\eta_x\right)^{\frac{2}{3}}} \tag{30}$$

where Sc_y und Re are defined by:

$$Sc_y = \frac{\eta_y}{D_y\rho_y} \text{ and } Re = \frac{\rho_y\,u\,d}{\eta_y} \tag{31}$$

5.1.2. Energy dissipation

The energy dissipation is a key parameter for breakage and coalescence frequency and propability calculations. In FLUENT, the energy dissipation is calculated for each numerical discretization cell in the whole domain. For turbulence modeling, the k-ε model is used, whereas the kinetic energy *k*, and its rate of dissipation are obtained from the following equations [30]:

$$\frac{\partial}{\partial t}(\rho k)+\frac{\partial}{\partial x_t}(\rho k u_t)=\frac{\partial}{\partial x_t}\left[\left(\eta+\frac{\eta_t}{\sigma_k}\right)\frac{\partial k}{\partial x_j}\right]+G_k-\rho\varepsilon \tag{32}$$

$$\frac{\partial}{\partial t}(\rho \varepsilon)+\frac{\partial}{\partial x_t}(\rho \varepsilon u_t)=\frac{\partial}{\partial x_t}\left[\left(\eta+\frac{\eta_t}{\sigma_k}\right)\frac{\partial \varepsilon}{\partial x_j}\right]+G_{1\varepsilon}\frac{\varepsilon}{k}(G_k)-G_{2\varepsilon}\rho\frac{\varepsilon^2}{k} \tag{33}$$

The generation of turbulence kinetic energy due to the mean velocity gradients is described by G_k:

$$G_k=-\frac{\rho\overline{u_i'u_j'}\left(\partial u_j\right)}{\partial x_t} \tag{34}$$

$G_{1\varepsilon}$ **and** $G_{2\varepsilon}$ are constants, which are defined as 1.44 and 1.92 respectively. The turbulent Prandtl numbers for the kinetic energy and the rate of dissipation are given by σ_k (=1.0) and σ_ε (=1.3) and define the ratio between momentum eddy and diffusivity.

The viscous sublayer is accounted by the enhanced wall treatment model, whereas the sublayer is fully resolved by refining the mesh that y^+, the wall distance unit, is approximately to 1.

6. Results and Discussion

The EFCE test system toluene-acetone-water (t-a-w) is used for the investigation, whereas acetone is the transition component between the aqueous and organic phase. The weight fraction of acetone in the aqueous phase is equal to 0.05. The physical properties of the test system are given in Table 1. The pilot plant RDC extraction column internal and external geometry dimensions are shown in Table 2 [6]. The operating conditions used: rotor speed is constant at 400 rpm and the volumetric flow rate for the continuous and dispersed phase is 40 l/hr and 48 l/hr, respectively.

Table 1. Physical properties of the chemical test system

Physical property		Physical property	
Density ρ_x	992.0 kg/m³	Viscosityη_x	1.134 E-03 Pa s
Density ρ_y	863.3 kg/m³	Viscosityη_y	0.566 E-03 Pa s
Interfacial tension	24.41E-03 Nm	Distribution coefficient	0.843 kg/kg

Table 2. Geometry and specifications of the RDC extraction column

Internal geometry		External geometry	
Compartment height	50 mm	Column height	4.40 m
Internal stator diameter	50 mm	Column diameter	0.08 m
Rotator diameter	45 mm	Inlet of dispersed phase	0.85 m
Rotating shaft diameter	10 mm	Inlet of continuous phase	3.80 m
Relative free cross sectional stator	0.40 m²/m²		

The values of droplet breakage and coalescence parameters for Coulaloglou and Tavlarides [19] (C_1-C_4) are estimated by solving the inverse problem for (t-a-w). Fig. (1) shows the optimization results for solving the inverse population balance problem by using the experimental data for both the holdup and the droplet diameter along the column height as reference value. The estimated parameters were C_1= 0.247, C_2= 0.078, C_3= 0.0351 and C_4= 1.33E11.

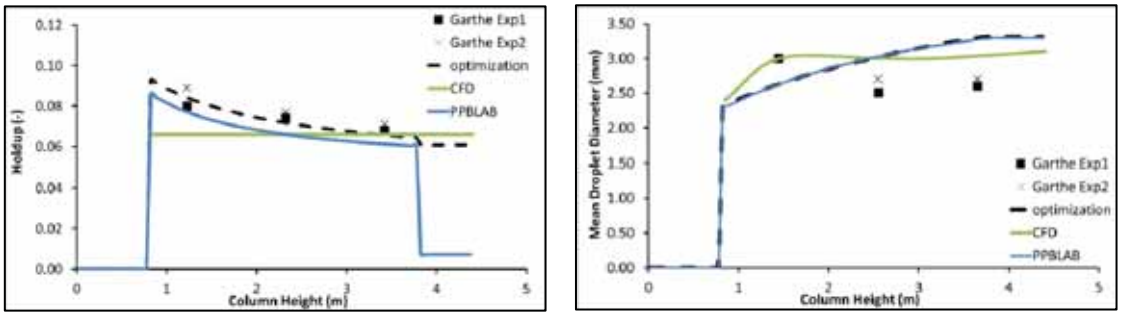

(a) (b)

Fig. 1. Optimization of breakage and coalescence parameters using the experimental data for the holdup and mean droplet diameter. a) Simulated mean holdup along column height; b) Simulated mean droplet diameter along the column height

Using these optimized parameters, CFD simulations were performed. The RDC extraction column is described by a numerical mesh, whereas the inflow and outflow zone was reduced in size to reduce the numerical effort. In both settling zones, the breakage and coalescence were neglected. The dispersed phase (organic phase) inlet is at the bottom, whereas the continuous phase enters the column at the top. Therefore, a velocity inlet is defined for both phases at the bottom of the column and the pressure outlet condition is used at the top.

The resulting CFD simulations for phase fraction, continuous phase velocity and droplet size in the bottom and the top of the column is shown in Fig. (2) and (3) respectively. The droplets accumulate underneath the first stator, which is shown in Fig. (2a). Two torus vortexes are formed by the stirrer (Fig. 2b), whereas Drumm (2009) [13] could only observe one vortex filling a compartment due to its lower compartment height. The upper vortex underlies a slight upward deviation due to the entering droplets.At the stirrer tip, the droplet size decreases due to the energy input(Fig. 2c). Underneath the stator, the droplets accumulate and coalesce, whereas in the lower part of the next compartment, higher droplet sizes can be observed. At the column top, the droplet size increased to approximated 3 mm (Fig. 3c), which leads to a slight changes in the phase fraction distribution (Fig. 3a). The two torus vortexesare formed,

whereas in this case, the center of the upper vortex is shifted due to the inflow of the continuous phase (Fig. 3b).

The droplet size was over predicted by the CFD simulation, whereas the phase fraction shows a good agreement to the measurements. It could be explained for the reason that the optimization was based on more on the phase fraction as integral value and not equally to the droplet size itself, also it is effected by the measuring position due to the measuring technique.

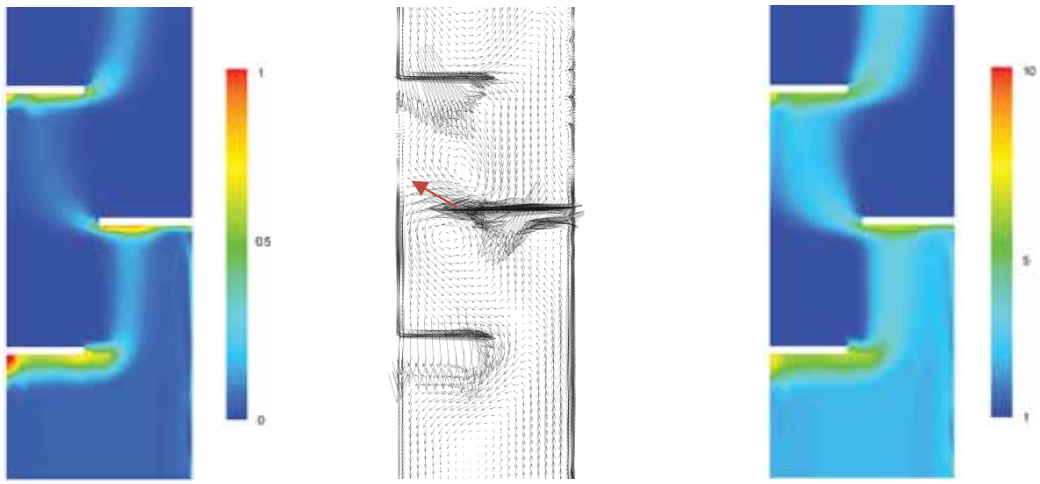

(a) (b) (c)

Fig. 2. CFD simulations at the bottom of extraction column for: (a) phase fraction (-), (b) continuous phase velocity (m/s) and (c) droplet size (mm)

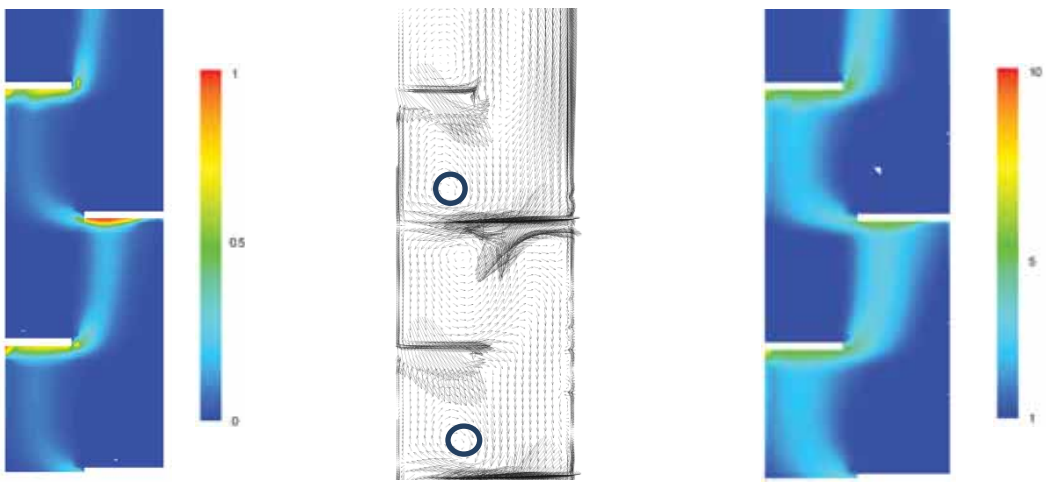

(a) (b) (c)

Fig. 3. CFD simulations at the top of the extraction column for: (a) phase fraction (-),(b) continuous phase velocity (m/s)and (c) droplet size (mm)

The resulted holdup and droplet size of the optimization, the CFD simulation and PPBLAB with mass transfer is compared to the experimental results shown in Fig. (1). The PPBLABsimulation of the droplet size fits to the one found by the optimization. The droplet size in the CFD simulation increases faster than the one found with the optimization tool. All simulations overpredict experimental droplet sizes at the upper measurement positions. An optimized droplet size instead leads to a correct prediction of the experimental holdup profile using the optimization algorithm and PPBLAB. For the CFD result, only an average value was taken for the active height, which underpredicts the holdup profile.

The concentration of acetone in the dispersed phase and continuous phase is compared to the experimental measurements in Fig. (4). However, the concentration of the continuous phase fit the experimental data and the dispersed phase values are underpredicted by the CFD simulation.The reason is that it requires more simulation time to research steady state.With three times longer simulation time in PPBLAB the concentration for both phases profiles were accurately predicted.

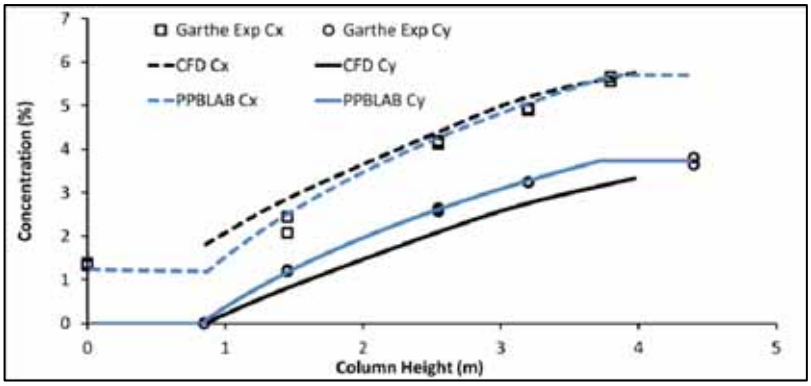

Fig. 4. Concentration profiles for continuous (C_x) and dispersed (C_y) phase along the column height.

7. Conclusions

A full pilot plant RDC extraction column was simulated based on the measurements of Garthe (2006) using a coupled CFD-DPBM-mass transfer model. As DPBM model, the one group population balance model, the One Primary and One Secondary Particle Model (OPOSPM) was used. In this work the OPOSPM is found to be a promising model for designing, simulating, controlling and optimizing a RDC extraction column.The required droplet interaction parameters in the breakage and coalescence model of Coulaloglou and Tavlarides were optimized using the inverse approach based on the experimental measurements of Garthe (2006) for droplet diameter and holdup along the column height. Mass transfer was accounted by the model of Kumar and Hartland (1999) for both the CFD and PPBLAB simulation. The results of the codes were compared to the experimental data.The droplet size was over predicted by the CFD code and PPBLAB, whereas the phase fraction shows a good agreement to the measurements. The concentration profile of the continuous phase fits to the experimental results; whereas the dispersed phase concentration is underpredicted (simulations in CFD require more time to reach a final steady state). The PPBLAB simulation indeed fits to the experimental values. Comparing the CFD and PPBLAB results, PPBLAB is able to predict the holdup, droplet size and concentration within minutes. On the other hand, PPBLAB is based and requires for each column type a set of experimental correlations to

determine e.g. the energy dissipation and back-mixing effects. The CFD in addition gives information about the local distribution of the droplets, local deviations of the hydrodynamics (e.g. the energy dissipation and back-mixing effects) dependent the inflow conditions of the phases into the active column part.

The optimization of parameters using the inverse tool is a promising technique to determine breakage and coalescence parameters for the specific models. It saves time due to a stable and fast optimization. The estimated parameters then can be used effectively as a basis for extraction column behavior prediction using CFD (FLUENT or OpenFOAM) and PPBLAB simulations.

Acknowledgements

The authors would like to acknowledge Fraunhofer Institute for Industrial Mathematics ITWM, Centre of Mathematical and Computational Modelling (CM)², DFG (Deutsche Forschungsgemeinschaft) and Max Buchner Research Foundation for the financial support.

References

[1] Attarakih M, Bart HJ, Lagar G L, Faqir N. LLECMOD: A Windows-based program for hydrodynamics simulation of liquid–liquid extraction columns. *Chem Eng Process* 2006;**45**:113–123.

[2] Attarakih M, Bart HJ, Steinmetz T, Dietzen M, Faqir N. LLECMOD: A Bivariate Population Balance Simulation Tool for Liquid-Liquid Extraction Columns. *Open Chem Eng J* 2008;**2**:10–34.

[3] Bart HJ, Hlawitschka M, Mickler M, Jaradat M, Didas S, Chen F, Hagen H. Tropfencluster – Analytik, Simulation und Visualisierung. Droplet Cluster – Analysis, Simulation and Visualization. *Chem Ing Tech* 2011;**83(7)**:965–978.

[4] Attarakih M, Al-Zyod S, Abu-Khader M, Bart HJ, Jildeh HB. PPBLAB: A new multivariate population balance environment for particulate system modeling and simulation. *Procedia Engineering* 2012, Accepted for publishingin the 20th International Congress of Chemical and Process Engineering, 25-29 August, Prague.

[5] Drumm C, Attarakih M, Hlawitschka M, Bart HJ. One-Group Reduced Population Balance Model for CFD Simulation of a Pilot-Plant Extraction Column. *Ind Eng Chem Res* 2010; **49(7)**:3442–3451.

[6] Garthe D. *Fluiddynamics and mass transfer of single particles and swarms of particles in extraction columns*. München:Dr. Hut; 2006.

[7] Ramkrishna D. *Population Balances: Theory and Applications to Particulate Systems in Engineering*. San Diego:*Academic Press*; 2000.

[8] Attarakih M, Bart HJ, Faqir N. Numerical solution of the bivariate population balance equation for the interacting hydrodynamics and mass transfer in liquid-liquid extraction columns. *Chem Eng Sci* 2006;**61(1)**:113–123.

[9] Kumar S, Ramkrishna D. On the solution of population balance equations by discretization—I. A fixed pivot technique. *Chem Eng Sci* 1996;**51(8)**:1311–1332.

[10] Kumar S, Ramkrishna D. On the solution of population balance equations by discretization—II. A moving pivot technique. *Chem Eng Sci* 1996;**51(8)**:1333–1342.

[11] JunWei S, ZhaoLin G, Yun XX. Advances in numerical methods for the solution of population balance equations for disperse phase systems. *Sci China Ser* B: *Chem* 2009;**52(8)**:1063–1079.

[12] Zhao H, Maisels A, Matsoukas T, Zheng C. Analysis of four Monte Carlo methods for the solution of population balances in dispersed systems. *Powder Technol* 2007;**173(1)**:38–50.

[13] Drumm C, Attarakih M, Bart H-J. Coupling of CFD with DPBM for an RDC extractor. *Chem. Eng. Sci.* 2009;**64**(4):721–732.

[14] Attarakih M, Drumm C, Bart HJ. Solution of the population balance equation using the sectional quadrature method of moments (SQMOM). *Chem Eng Sci* 2009;**64(4)**:742–752.

[15] Attarakih M, Jaradat M, Bart HJ, Kuhnert J, Drumm C, Tiwari S, Sharma VK, Klar A. A multivariate Sectional Quadrature Method of moments for the Solution of the Population Balance Equation.In: Pierucci S., Buzzi Ferraris G., editors. *Computer Aided Chemical Engineering: 20th European Symposium on Computer Aided Process Engineering, Elsevier* 2010.

[16] Attarakih M, Jaradat M, Hlawitschka MW, Bart HJ, Kuhnert J. Integral Formulation of Solution of the Population Balance Equation using the Cumulative QMOM. In:Pistikopoulos EN, Georgiadis MC, Kokossis AC, editors.*Computer Aided Chemical Engineering: 21st European Symposium on Computer Aided Process Engineering, Elsevier* 2011;**29**:81–85.

[17] Attarakih MM, Kuhnert J, Wächtler T, Abu-Khader M, Bart HJ. Solution of the Population Balance Equation using the Normalized QMOM (NQMOM). *8th International Conference on CFD in Oil & Gas, Metallurgical and Process Industries* 2011, 21-23 June, Trondheim, Norway.

[18] Attarakih MM, Jaradat M, Drumm C, Bart HJ, Tiwari S, Sharma VK, Kuhnert J, Klar A. Solution of the Population Balance Equation using the One Primary One Secondary Particle Method (OPOSPM). *Comp Aid Chem Eng* 2009;**26**:1333-1338

[19] Coulaloglou C, Tavlarides L. Description of interaction processes in agitated liquid-liquid dispersions. *Chem Eng Sci* 1977;**32(11)**:1289–1297.

[20] Godfrey JC, Slater MJ. *Liquid-liquid extraction equipment*. Chicheste: John Wiley &Sons; 1994.

[21] Liao Y, Lucas D. A literature review of theoretical models for drop and bubble breakup in turbulent dispersions. *Chem Eng Sci* 2009;**64(15)**:3389–3406.

[22] Sovová H. Breakage and coalescence of drops in a batch stirred vessel-II comparison of model and experiments. *Chem Eng Sci* 1981;**36(9)**:1567–1573.

[23] Casamatta G, Vogelpohl A. Modelling of Fluid Dynamics and Mass Transfer in Extraction Columns. *German chemical engineering* 1985;**8(2)**:96–103.

[24] Laso M, Steiner L, Hartland S. Dynamic simulation of liquid-liquid agitated dispersions-I. Derivation of a simplified model. *Chem. Eng. Sci.* 1987;**42(10)**:2429–2436.

[25] Lane G, Schwarz M, Evans G. Numerical Modelling of Gas–Liquid Flowin Stirred Tanks. *Chem Eng Sci* 2005;**60**:2203–2214.

[26] Liao Y, Lucas D. A literature review on mechanisms and models for the coalescence process of fluid particles. *Chem. Eng. Sci.* 2010; **65(10)**: 2851–2864.

[27] Tsouris C, Tavlarides L L. Breakage and coalescence models for drops in turbulent dispersions. *AlChE J* 1994;**40(3)**:395–406.

[28] Jildeh H B, Attarakih M, Mickler M, Bart H-J. An Online Inverse Problem for the Simulation of Extraction Columns using Population Balances. *Accepted for publishing in the proceeding of 22nd European Symposium on Computer-Aided Process Engineering* 2012, 17-20 June, London.

[29] Jildeh H B, Attarakih M, Bart H-J. Coalescence Parameter Estimation in Liquid Extraction Column using OPOSPM. *Accepted for publishing in the proceeding of 11th International Symposium on Process Systems Engineering* 2012, 15-19 July, Singapore.

[30] Fluent Inc. Fluent 6.3 manual 2006. Avaliable online http://hpce.iitm.ac.in/website/Manuals/Fluent_6.3/Fluent.Inc /fluent6.3/help/index.htm, (accessed on 26 April 2012).

[31] Kumar A, Hartland S. Correlations for prediction of mass transfer coefficients in single drop systems and liquid-liquid extraction columns. *Chem. Eng. Res. Des.*1999;77:372-384.